

# Electrode Work Function Reduction by Polyethylenimine Interlayers: Choice of Solvent and Residual Solvent Removal for Superior Functionality

Sujitkumar Bontapalle, Andreas Opitz, Raphael Schlesinger, Seth R. Marder, Susy Varughese, and Norbert Koch\*

Ultrathin polyethylenimine (PEI) interlayers are frequently used to reduce the work function of electrode materials; however, to exploit the full potential of this material for application in optoelectronic devices, further fundamental understanding is required. Here, it is demonstrated that intermixing of PEI deposited from water solution onto the conductive polymer poly(3,4-ethylene-dioxythiophene) (PEDOT):polystyrene sulfonate can be avoided by using anhydrous butanol as solvent. At the same time, this choice of solvent prevents de-doping of PEDOT and preserves the electrode's transparency. For inorganic electrode materials, i.e., ZnO and graphite, it is demonstrated that residual solvent in PEI films, present even after annealing in inert gas atmosphere, leads to significant surface dewetting, and thus inhomogeneity in terms of the morphology and work function. However, annealing in ultrahigh vacuum removes residual solvent, establishes homogenous surface coverage with PEI, and allows one to achieve the maximum work function reduction. For the transparent electron transport material ZnO, a record low work function value of 2.3 eV is achieved, which can enable the formation of ohmic contacts to most semiconductors.

like polyethylenimine (PEI) and ethoxylated PEI (PEIE) reduce the electrode work function and thus improve electron injection/extraction.<sup>[1]</sup> Due to the presence of ethoxy groups, PEIE has a higher solubility in water at room temperature in comparison to PEI. Such interlayers were subsequently used to improve the performance of all-polymeric solar cells,<sup>[1,2]</sup> inverted OPVCs,<sup>[3–7]</sup> OLEDs,<sup>[8–10]</sup> and perovskite solar cells.<sup>[11,12]</sup>

Among other electrode materials, PEI and its derivative were used to reduce the work function of the water-soluble poly(3,4-ethylenedioxythiophene):polystyrene sulfonate mixture (PEDOT:PSS), a prototypical conductive polymer, which typically has a rather high work function. However, when using water as solvent to deposit PEI onto PEDOT:PSS, the conductivity of the polymer film was strongly reduced.<sup>[13]</sup> Other solvents, such as methoxyethanol and isopropyl alcohol, or upon additional doping of the film by

sulfuric acid helped overcoming the drawback of reduced conductivity.<sup>[2,6]</sup> Notably, even vapor exposure of PEDOT:PSS to PEI solution resulted in a conductivity loss due to the presence of short ethyleneimine oligomers in PEI.<sup>[13]</sup> On other electrodes, such as indium tin oxide (ITO),<sup>[1]</sup> thin PEI interlayers deposited from water solution exhibited poor film morphology, most notably incomplete coverage. PEI from aqueous solution also exhibited similar poor morphology on weakly interacting and hydrophobic surfaces like highly oriented pyrolytic graphite (HOPG) and mica.<sup>[14,15]</sup> Furthermore, it was shown that the thickness of PEI films, typically below 10 nm, plays a critical

## 1. Introduction

The ability to control the work function of electrodes in electronic devices has contributed significantly to the enhancement of device performance by reducing ohmic losses at the interface to the semiconductor. Modifying an electrode's work function via insertion of thin interlayers has been demonstrated to be an effective strategy to optimize the interfacial energy level alignment and thereby to achieve superior charge injection/extraction in organic light-emitting diodes (OLEDs) and organic photovoltaics cells (OPVCs). To that end, interlayers of aliphatic amines

S. Bontapalle, Prof. S. Varughese  
Department of Chemical Engineering  
Indian Institute of Technology Madras  
Chennai, Tamil Nadu 600036, India



The ORCID identification number(s) for the author(s) of this article can be found under <https://doi.org/10.1002/admi.202000291>.

© 2020 The Authors. Published by WILEY-VCH Verlag GmbH & Co. KGaA, Weinheim. This is an open access article under the terms of the Creative Commons Attribution License, which permits use, distribution and reproduction in any medium, provided the original work is properly cited.

DOI: 10.1002/admi.202000291

Dr. A. Opitz, Dr. R. Schlesinger, Prof. N. Koch  
Institut für Physik & IRIS Adlershof  
Humboldt-Universität zu Berlin  
Berlin 10099, Germany  
E-mail: [norbert.koch@physik.hu-berlin.de](mailto:norbert.koch@physik.hu-berlin.de)

Prof. S. R. Marder  
School of Chemistry and Biochemistry and Center for  
Organic Photonics and Electronics (COPE)  
Georgia Institute of Technology Atlanta  
Atlanta, GA 30332, USA

Prof. N. Koch  
Helmholtz-Zentrum Berlin für Materialien und Energie GmbH  
Berlin 14109, Germany

role for device performance, and should thus be controlled precisely.<sup>[16]</sup> Hence, it is important to have an interlayer that appropriately modifies the work function without detrimentally changing the underlying electrode properties like bulk conductivity and morphology, yet yielding continuous, thin and smooth films to enable an optimized overall device performance.

This study investigates the morphology and the electronic properties of PEI treatment on different electrode materials, which range from the conductive polymer mixture PEDOT:PSS over zinc oxide (ZnO) as low work function metal oxide to HOPG as inert and hydrophobic material. Two different solvents were used to apply the PEI treatment. Water (H<sub>2</sub>O) has a reasonable dissolving power for PEI at elevated temperature and butanol even at room temperature. The morphology was altered after treatment by annealing under ultrahigh vacuum conditions. We analyzed the morphology and the electronic properties in dependence on the applied solvent and the annealing procedure.

## 2. Results

### 2.1. PEI on PEDOT:PSS

As PEDOT:PSS is processed from water-based solution, using water as solvent for subsequently deposited PEI-H<sub>2</sub>O may not be ideal. Anhydrous butanol (BuOH) was thus used in addition, processed under inert glovebox atmosphere PEI-BuOH. Due to the low solubility of PEI in H<sub>2</sub>O at room temperature, the PEI solution was spin coated at slightly elevated temperature (yet below 80 °C, the temperature of the solution during stirring).

Figure 1a shows the surface morphology of a bare PEDOT:PSS film and those with PEI spin coated on top, from BuOH and H<sub>2</sub>O. Whereas the surface roughness of bare and PEI-BuOH-treated PEDOT:PSS films (RMS ≈ 2 nm) is comparable, the roughness is significantly increased for the PEI-H<sub>2</sub>O-treated PEDOT:PSS film (RMS ≈ 6 nm). The optical absorption of the samples is shown in Figure 1b. The bare PEDOT:PSS films exhibit the typical broad absorption feature above 1140 nm, which is related to the absorption of positively charged PEDOT chains.<sup>[17]</sup> The weak absorption peak around 600 nm arises from the absorption of neutral PEDOT segments. Upon PEI-BuOH treatment, only minor changes of the absorption are observed. In contrast, the treatment

of PEDOT:PSS film with water-based PEI solution reduces strongly the absorption of the charged PEDOT and the absorption peak from neutral segments is increased.<sup>[13]</sup> The decharging of PEDOT was reported to be accompanied by the formation of protonated amine groups of PEI.<sup>[1,13]</sup> Absorption features of PSS and PEI are absent in the examined spectra range.

To assess the work function of the samples, the secondary electron cutoff (SECO) was measured with photoelectron spectroscopy spectra displayed in Figure 2a. The bare PEDOT:PSS film has a work function of 4.9 eV, the PEI-treated samples exhibit a reduced work function of 4.0–4.1 eV. Apparently, the work function of PEI/PEDOT:PSS seems to be independent on the choice of solvent, despite the notable differences in morphology and absorption.

The spectra taken for the nitrogen 1s core level are shown in Figure 2b. A PEI-BuOH-treated PEDOT:PSS film shows two distinct peaks. The peak at lower binding energy is related to N atoms in neutral amine groups, whereas the higher binding energy one belongs to protonated amine groups.<sup>[1]</sup> The measured spectra for PEI-BuOH treatment are comparable to the spectra of PEI on PEDOT:PSS prepared with low pH values, as found in literature.<sup>[1]</sup> The appearance of the high binding energy peak after PEI-H<sub>2</sub>O treatment is rather broad and unspecific, as observed before for PEI:PSS mixtures.<sup>[18]</sup>

By treating the PEDOT:PSS film with PEI from solution, protonation of amine groups in the PEI was reported. For PEI-BuOH treatment, this is more directly detected at the surface in our N 1s spectra. Together with the minor changes in optical absorption, we conclude on the presence of PEI only at the very surface of PEDOT:PSS when deposited from BuOH solution. The strong change in absorption when PEI is applied from H<sub>2</sub>O solution strongly indicates its diffusion deep into the PEDOT:PSS film. The ionic polymers are then PEI and PSS and decharging of PEDOT takes place. This results in the reduced conductivity as was observed for PEI-H<sub>2</sub>O-treated PEDOT:PSS films in literature.<sup>[13]</sup> The PEI-BuOH treatment gives a similar work function reduction as the PEI-H<sub>2</sub>O treatment, but affects only the surface of the conductive polymer film. A modified surface arrangement of the PEDOT:PSS polymer chains from coiled to more linear was observed upon treatment with alcohols including BuOH, which might be related to the lower dielectric constant of BuOH compared to H<sub>2</sub>O.<sup>[19,20]</sup> This surface-limited interaction of the solvent with the PEDOT:PSS film would also restrict the charge exchange

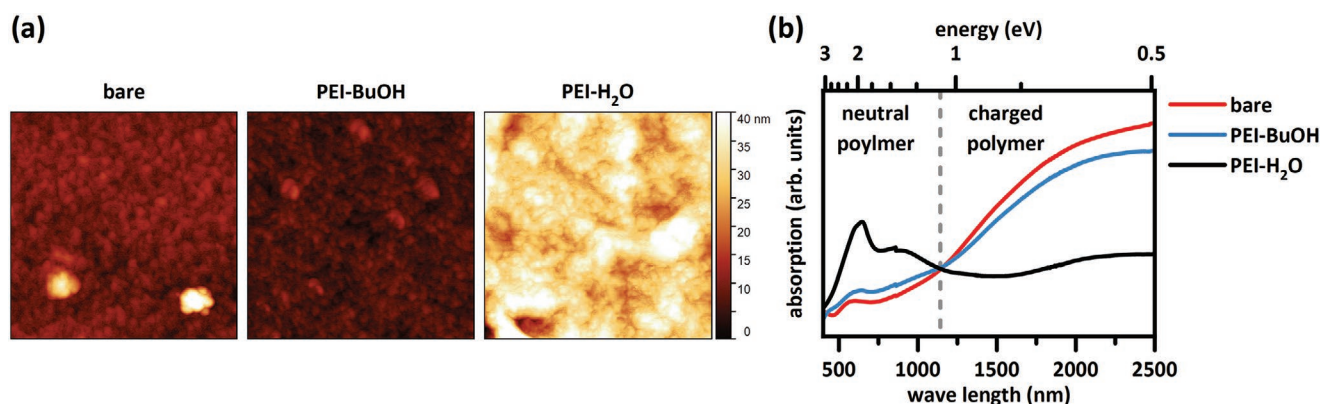


**Figure 1.** Scanning force micrographs a) and optical absorption spectra b) for a bare PEDOT:PSS film, and PEDOT:PSS films after spin coating of PEI from BuOH (PEI-BuOH) and H<sub>2</sub>O (PEI-H<sub>2</sub>O) solution. The scan size of the images is 3 × 3 μm<sup>2</sup>.

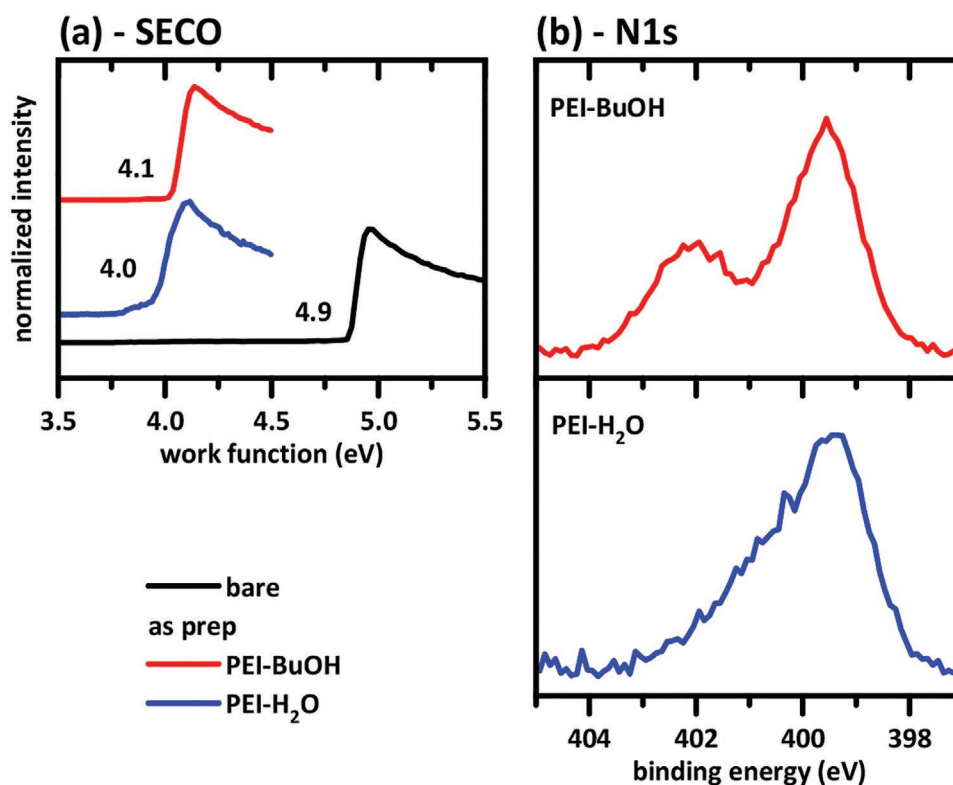


**Figure 2.** a) SECO spectra to determine the work function for bare PEDOT:PSS, and PEDOT:PSS after spin coating of PEI from BuOH (PEI-BuOH) and H<sub>2</sub>O (PEI-H<sub>2</sub>O). b) N 1s core level spectra for PEDOT:PSS films after PEI-BuOH and PEI-H<sub>2</sub>O treatment.

between PEDOT and PEI to near-surface region. With this, the bulk conductivity should remain unchanged, which is certainly an advantage of PEI-BuOH treatment over PEI-H<sub>2</sub>O treatment.

## 2.2. PEI on ZnO and HOPG

In contrast to PEDOT:PSS, no penetration of solution-deposited PEI into ZnO and HOPG is expected. ZnO is often used as solution-processible and transparent electron injecting electrode,<sup>[21]</sup> and HOPG is a model system for the transparent and highly conductive graphene.<sup>[22,23]</sup>

The as-prepared PEI films are very inhomogeneous as seen from the respective height and phase images shown in **Figure 3**. Both PEI-H<sub>2</sub>O and PEI-BuOH give rough PEI films and a clear material contrast is detected from phase images, suggesting incomplete surface coverage. PEI-BuOH-treated ZnO shows surface height modulation on the  $\mu\text{m}$ -scale, probably due to aggregation of PEI, and comparably well-defined small clusters for PEI-H<sub>2</sub>O-treated ZnO. PEI forms large clusters with a height up to 150 nm on HOPG. Graphite is hydrophobic, which apparently prevents the surface from being wetted by PEI. This was observed before also for PEIE deposited from aqueous solution.<sup>[14]</sup> The better as-prepared PEI distribution on ZnO is due to the surface hydroxyls present on the metal oxide at room temperature.

After annealing at 150 °C in ultrahigh vacuum, the film corrugation is substantially reduced for ZnO, and the material contrast in the phase images vanishes, suggesting complete coverage with PEI. The film corrugation is also greatly

decreased for PEI on HOPG. However, complete coverage is not achieved as indicated by the remaining phase contrast in the micrographs. Distinct differences between H<sub>2</sub>O and BuOH as solvents for PEI are not observed after annealing.

The morphology change upon annealing in vacuum has a remarkable impact on the work function. The work function of bare ZnO and HOPG is 4.0 and 4.5 eV, respectively, as shown in **Figure 4a** from SECO measurements. These values are reduced to 3.1–3.4 eV upon deposition of PEI. After annealing at 150 °C in ultrahigh vacuum, the work function is further reduced to 2.3–2.7 eV. This work function evolution can be understood from the observed morphology change. The work function of as-prepared PEI-coated ZnO and HOPG is in between the values of the bare substrates and the substantially more homogeneous PEI films (after annealing). The work function of multi-component surfaces is an average of the local work function values of the individual components.<sup>[24]</sup>

An eventual residual solvent content of the PEI films on ZnO was analyzed by an inspection of the oxygen 1s core level, depicted in **Figure 4b**. The bare ZnO substrate shows one asymmetric peak, with the surface hydroxyls giving rise to the asymmetric tail toward higher binding energy. The as-prepared PEI-H<sub>2</sub>O film on ZnO shows a distinct shoulder at higher binding energy, which can indeed be related to residual water.<sup>[25]</sup> This component is present with lower intensity also for the sample prepared from PEI-BuOH inside a glovebox. It may thus be derived from residual BuOH. The hygroscopic PEI can attract water also from the atmosphere inside the inert gas glovebox, which could also contribute to the peak. However, the solvent-related



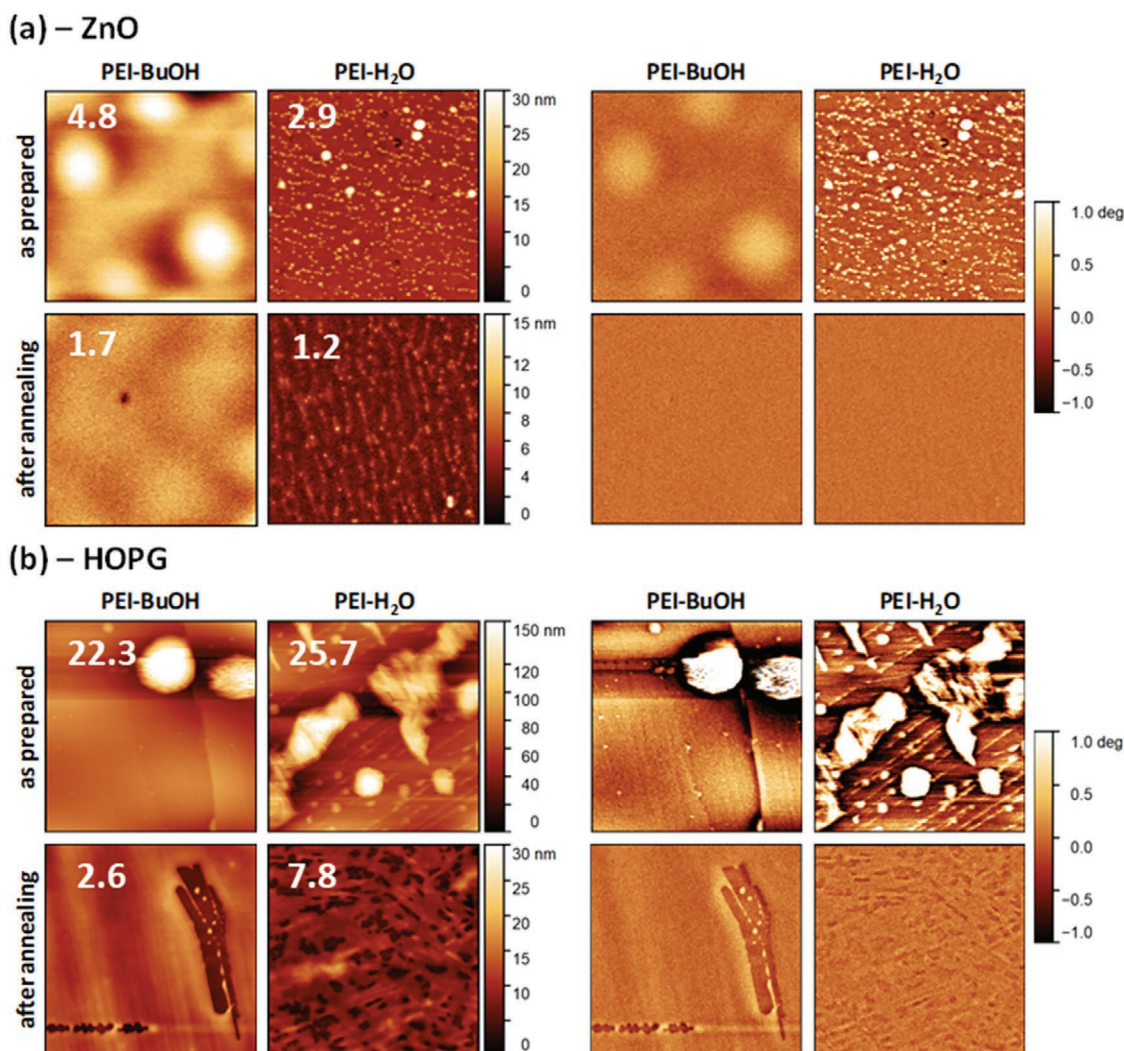


**Figure 3.** Scanning force micrographs for PEI deposited on top of a) ZnO and b) HOPG from BuOH (PEI-BuOH) and H<sub>2</sub>O (PEI-H<sub>2</sub>O) solution, as prepared and after annealing. The surface morphology is shown in the left column (scan size  $7 \times 7 \mu\text{m}^2$ ), the corresponding phase contrast is in the right column. The numbers in the upper left corner of morphology images (left column) are the corresponding root-mean-square roughness values.

component of the O 1s spectra is completely gone after annealing at 150 °C in ultrahigh vacuum, for both solvents.

Note, the PEI films were annealed during the preparation process already at 140 °C in the inert gas glovebox (PEI-BuOH) or at ambient conditions (PEI-H<sub>2</sub>O) to remove residual solvent. However, only annealing of PEI films at 150 °C in ultrahigh vacuum removed solvent completely from the film. At the same time, this improved the surface coverage and film homogeneity, in hand with a significant further work function reduction. The improved coverage of PEI films on the substrate due to annealing in vacuum seems to be related to the removal of solvent. The presence of a low amount of solvent in the PEI film may result, due to low solubility and a delicate surface energy balance, to dewetting and aggregate formation of PEI. After annealing, residual solvent is gone and the system consists only of substrate and PEI, which improves the wettability and coverage. Both points, the removal of solvent from the PEI film and the improved film coverage, result in the lowest work function. The differences between H<sub>2</sub>O and

BuOH as solvent for PEI are negligible for the nonpolymeric electrode materials.

**Figure 5** gives a compilation of the work function values of PEI films in dependence of the respective substrate work function. The work function of all substrates is reduced by spin coating the PEI from H<sub>2</sub>O and BuOH approximately by 0.93 eV. After annealing at 150 °C in ultrahigh vacuum, the work function is reduced further to about 1.65 eV below the substrate work function. The later reduction of the work function is related to the removal of solvent from the PEI films and an improved coverage with PEI. It is worth noting that the work function of PEI on inorganic substrates (ZnO and HOPG) and that of PEI-treated PEDOT:PSS films exhibit the same trend for the as-prepared case. Even if the details of film morphology are different for the applied solvents (H<sub>2</sub>O and BuOH), the achieved work function is independent of the choice of the solvent. Additionally, the work function for PEIE films is shown in Figure 5 as taken from ref. [1]. Whereas in the here presented study the work function change seems to be constant for each preparation

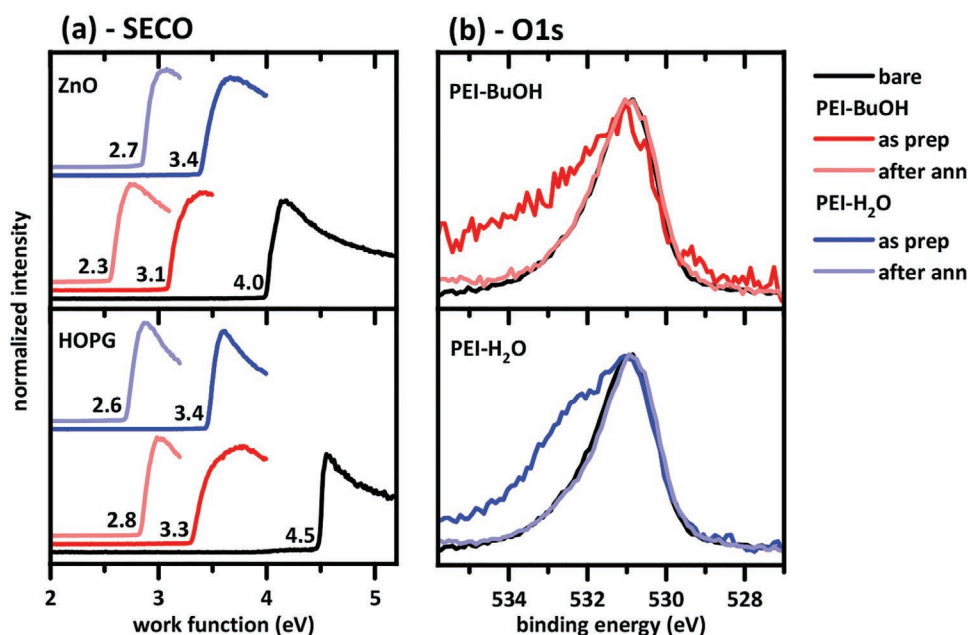


**Figure 4.** a) SECO spectra to determine the work function for bare ZnO and HOPG, and for PEI deposited on top from BuOH (PEI-BuOH) and H<sub>2</sub>O (PEI-H<sub>2</sub>O) solution, as prepared and after annealing. b) O 1s core level spectra of bare ZnO and after PEI deposition from BuOH (PEI-BuOH) and H<sub>2</sub>O (PEI-H<sub>2</sub>O) solution, as prepared and after annealing.

step, the final work function is similar for all samples given in the reference. This might be related also to residual solvent in PEIE. We also note that the work function achieved under non-UHV condition annealing (e.g., high vacuum, inert gas box) will depend on the residual water content of the atmosphere, as we observed a work function increase by up to 1 eV when exposing a UHV-annealed PEI/ZnO film to  $\approx 10^{-5}$  mbar water vapor for a few minutes. Further studies could address differences between films of linear PEI and branched ethoxylated PEI, as well as the effect of solvent incorporation.

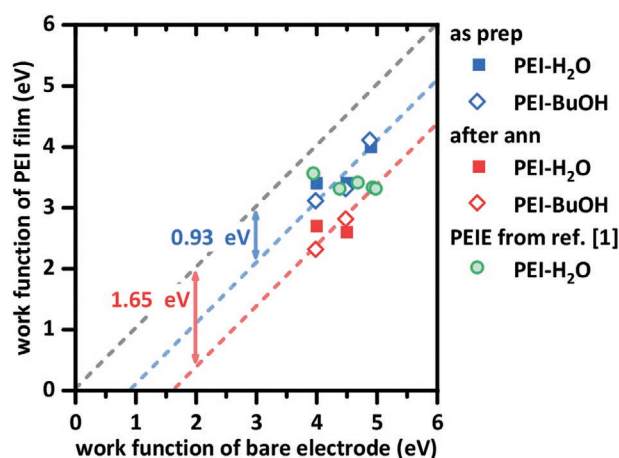


**Figure 5.** Compilation of measured work function values of PEI films in dependence on the work function of the respective bare substrate, for preparation from BuOH (PEI-BuOH) and H<sub>2</sub>O (PEI-H<sub>2</sub>O) solution, and as prepared (blue data points) and after annealing (red data points). Additionally, the corresponding data for PEIE from ref. [1] are included (green data points).

### 3. Conclusion

The influence of preparation conditions of PEI films to reduce the work function of electrode materials (PEDOT:PSS, ZnO and HOPG) was investigated. For the conductive polymer PEDOT:PSS, we find that PEI deposited from water solution leads to very significant diffusion of PEI into the PEDOT:PSS film and dedoping of PEDOT. In contrast, when PEI is deposited from butanol, negligible diffusion and dedoping occur, and a work function of  $\approx 4$  eV is achieved. On the inorganic electrode materials ZnO and HOPG, PEI deposited from either solvent leads to poor surface coverage with PEI due to dewetting. This found to be due to residual solvent in PEI films, present even after annealing in inert gas atmosphere. Only annealing in (ultra)high vacuum eliminates residual solvent, which significantly enhances PEI film homogeneity and results in very low work function values. The lowest achieved value here is 2.3 eV for PEI on ZnO after annealing in vacuum. Our results highlight the importance of—often unnoticed—residual solvent content in polymer films and the need for rigorous control of this parameter to optimize the resulting film properties for the demands in devices.

### 4. Experimental Section

PEDOT:PSS (purchased from Ossila Inc. as PH1000) films were formed by spin coating on ITO-coated glass slides. Subsequently, the samples were annealed at 120 °C for 10 min to remove water. ZnO crystals (oxygen-terminated ZnO(000-1), purchased from CrysTec GmbH) were cleaned by annealing at 1100 °C for 4 h in a hot furnace in air. HOPG (purchased from Optigraph GmbH) was prepared by freshly cleaving the crystal using adhesive tape.

PEI was received from Sigma-Aldrich Chemie GmbH as linear polymer with a molecular weight of 5000 Da. To dissolve PEI in water (PEI-H<sub>2</sub>O),

the solution was continuously stirred using magnetic pellets at 80 °C on a hot plate. Additionally, anhydrous butanol was used to dissolve PEI (PEI-BuOH). This solution was held at room temperature. PEI films were prepared by spin coating the PEI-BuOH and the hot PEI-H<sub>2</sub>O solutions onto the respective substrates at 5000 rpm for 60 s and subsequent annealing at 140 °C for 10 min on a hot plate. For PEI-H<sub>2</sub>O samples, this procedure was carried out in ambient conditions, whereas for PEI-BuOH samples this was done in a nitrogen-filled inert-gas glovebox. All samples were transferred to an ultrahigh vacuum chamber for photoelectron spectroscopy measurements. This transfer for the sample prepared by PEI-BuOH proceeded without exposing the samples to air. Characterization at this stage was referred to “as prepared” in the following. Samples were also annealed in ultrahigh vacuum up to 150 °C. Post annealing measurements were referred to as “after annealing.”

Photoelectron spectroscopy was performed with excitation from He discharge lamp (HeI, excitation energy 21.1 eV) and from Al K $\alpha$  X-ray (1486.3 eV) source. The energy of the emitted electrons was characterized by a hemispherical analyser EA 125 (Scienta Omicron GmbH). The work function was determined for all samples by measuring the SECO. The morphology was investigated after photoelectron spectroscopy measurements by scanning force microscopy with a Dimension Icon in peak force tapping mode (Bruker Co.). UV-vis–near-infrared absorption spectra were collected for samples prepared with PEDOT:PSS films using a Lambda 950 spectrophotometer (Perkin Elmer Inc.).

## Acknowledgements

S.B. and A.O. contributed equally to this work. This work was supported by the Deutsche Forschungsgemeinschaft (SFB951, project number 182087777). S.B. acknowledges research fellowship from Ministry of Human Resource Development (Government of India) and travel grant from Alumni association IIT Madras (India). S.R.M. acknowledges the Alexander von Humboldt Foundation for its generous support of a Senior Research Award to facilitate the collaborative activities described herein. A.O. is grateful for discussion with Ellen Moons (University of Karlstad, Sweden).

## Conflict of Interest

The authors declare no conflict of interest.

## Keywords

electrodes, polyethylenimine interlayers, work function

Received: February 20, 2020

Revised: March 21, 2020

Published online: April 19, 2020

- [1] Y. Zhou, C. Fuentes-Hernandez, J. Shim, J. Meyer, A. J. Giordano, H. Li, P. Winget, T. Papadopoulos, H. Cheun, J. Kim, M. Fenoll, A. Dindar, W. Haske, E. Najafabadi, T. M. Khan, H. Sojoudi, S. Barlow, S. Graham, J.-L. Bredas, S. R. Marder, A. Kahn, B. Kippelen, *Science* **2012**, 336, 327.
- [2] Z. Li, Y. Liang, Z. Zhong, J. Qian, G. Liang, K. Zhao, H. Shi, S. Zhong, Y. Yin, W. Tian, *Synth. Met.* **2015**, 210, 363.
- [3] P. Li, G. Wang, L. Cai, B. Ding, D. Zhou, Y. Hu, Y. Zhang, J. Xiang, K. Wan, L. Chen, K. Alameh, Q. Song, *Phys. Chem. Chem. Phys.* **2014**, 16, 23792.
- [4] H. Kang, S. Hong, J. Lee, K. Lee, *Adv. Mater.* **2012**, 24, 3005.
- [5] F. C. Wu, K. C. Tung, W. Y. Chou, F. C. Tang, H. L. Cheng, *Org. Electron.* **2016**, 29, 120.
- [6] Z. Li, F. Qin, T. Liu, R. Ge, W. Meng, J. Tong, S. Xiong, Y. Zhou, *Org. Electron.* **2015**, 21, 144.
- [7] B. A. E. Courtright, S. A. Jenekhe, *ACS Appl. Mater. Interfaces* **2015**, 7, 26167.
- [8] Y. H. Kim, T. H. Han, H. Cho, S. Y. Min, C. L. Lee, T. W. Lee, *Adv. Funct. Mater.* **2014**, 24, 3808.
- [9] S. Stolz, M. Scherer, E. Mankel, R. Lovrinčić, J. Schinke, W. Kowalsky, W. Jaegermann, U. Lemmer, N. Mechau, G. Hernandez-Sosa, *ACS Appl. Mater. Interfaces* **2014**, 6, 6616.
- [10] S. Stolz, Y. Zhang, U. Lemmer, G. Hernandez-Sosa, H. Aziz, *ACS Appl. Mater. Interfaces* **2017**, 9, 2776.
- [11] K. M. Kim, S. Ahn, W. Jang, S. Park, O. O. Park, D. H. Wang, *Sol. Energy Mater. Sol. Cells* **2018**, 176, 435.
- [12] S. Dong, Y. Wan, Y. Wang, Y. Yang, Y. Wang, X. Zhang, H. Cao, W. Qin, L. Yang, C. Yao, Z. Ge, S. Yin, *RSC Adv.* **2016**, 6, 57793.
- [13] S. Fabiano, S. Braun, X. Liu, E. Weverberghs, P. Gerbaux, M. Fahlman, M. Berggren, X. Crispin, *Adv. Mater.* **2014**, 26, 6000.
- [14] M. Schneider, M. Brinkmann, H. Möhwald, *Macromolecules* **2003**, 36, 9510.
- [15] M. Fleischer, C. Schmuck, *Chem. Commun.* **2014**, 50, 10464.
- [16] T. Davidson-Hall, H. Aziz, *Nanoscale* **2018**, 10, 2623.
- [17] J. Gustafsson, B. Liedberg, O. Inganäs, *Solid State Ionics* **1994**, 69, 145.
- [18] Z. Lin, J. Chang, J. Zhang, C. Jiang, J. Wu, C. Zhu, *J. Mater. Chem. A* **2014**, 2, 7788.
- [19] D. Alemu, H.-Y. Wei, K.-C. Ho, C.-W. Chu, *Energy Environ. Sci.* **2012**, 5, 9662.
- [20] M. R. Lenze, N. M. Kronenberg, F. Würthner, K. Meerholz, *Org. Electron.* **2015**, 21, 171.
- [21] S. Höfle, A. Schienle, M. Bruns, U. Lemmer, A. Colmann, *Adv. Mater.* **2014**, 26, 2750.
- [22] Y. Song, S. Chang, S. Gradecak, J. Kong, *Adv. Energy Mater.* **2016**, 6, 1600847.
- [23] H. Park, J. A. Rowehl, K. K. Kim, V. Bulovic, J. Kong, *Nanotechnology* **2010**, 21, 505204.
- [24] T. Schultz, T. Lenz, N. Kotadiya, G. Heimel, G. Glasser, R. Berger, P. W. M. Blom, P. Amsalem, D. M. de Leeuw, N. Koch, *Adv. Mater. Interfaces* **2017**, 4, 1700324.
- [25] B. Hornetz, H.-J. Michel, J. Halbritter, *J. Mater. Res.* **1994**, 9, 3088.